https://doi.org/10.1016/j.scriptamat.2018.10.006


# Elastic modulus change and its relation with glass-forming ability and plasticity in bulk metallic glasses

Ming Yang[a], Xiongjun Liu[a], Yuan Wu[a], Hui Wang[a], Jianbiao Wang[b], Haihui Ruan[b,*], Zhaoping Lu[a,*]

[a]State Key Laboratory for Advanced Metals and Materials, University of Science and Technology Beijing, Beijing 100083, China

[b]Department of Mechanical Engineering, The Hong Kong Polytechnic University, Hung Hom, Kowloon, Hong Kong

## Abstract

In this work, we revealed the intrinsic relation between the modulus change upon heating and macroscopic properties such as glass-forming ability (GFA) and room-temperature plasticity in various metallic glasses. Specifically, GFA and plasticity can respectively be related to the softening rate right above the glass transition temperature ($T_g$) and the degree of sub-$T_g$ relaxation. These relations can be understood in terms of the unified picture of potential energy barrier crossing. Above $T_g$, the faster barrier crossing leads to the larger softening rate and the higher tendency of crystallization; below $T_g$, the easier local rearrangement brings about the larger plasticity.

**Keywords:** Metallic glasses, Modulus change, Atomic relaxation, Softening rate, Room-temperature plasticity

*Corresponding author:
Haihui Ruan (hhruan@polyu.edu.hk) or Zhaoping Lu (luzp@ustb.edu.cn)

Bulk metallic glasses (BMGs) have attracted extensive attention because of their fundamental role in understanding glass nature and the potential applications as structural materials [1, 2]. Unlike crystalline materials, the atomic packing inside BMGs lacks the translational order. Consequently, it is difficult to directly observe the atomic arrangement and its evolution via either crystallography-based microscopy or diffraction methods. Therefore, the atomic structure-property relationship is still missing although substantial progress has been made in the field of BMGs.

Instead, time-temperature dependences of physical properties were utilized to probe the underlying glass nature and the evolution of atomic arrangement when BMGs are subjected to heating and/or loading. Compared with other physical properties such as susceptibility [3], conductivity [4], density [5] and heat capacity [6], elastic modulus is supposed to more directly related to atomic bonding and more sensitive to time and temperature [7]. For example, the elastic modulus of Pd-Cu-Si MGs increased by about 30% when it was cooled from crystallization temperature $T_x$ to room temperature. Nevertheless, the same heat treatment only led to 0.3% increase of the density and 1.5% increase even after full crystallization [8]. The large change in the Young's modulus does not arise only from densification but also a consequence of the rearrangement of atoms and the chemical short-range ordering [9]. However, even though elastic modulus reflects the property directly associated with inherent static structure of BMGs, it is surprising to note that investigation of structural relaxation is still largely based on calorimetry or enthalpy variation [10, 11].

In this work, we attempt to investigate structural relaxation of BMGs through

in-situ monitoring the variation of elastic modulus with temperature by the impulse excitation technique (IET) which is based on the mechanical vibration of a solid body by means of a slight impact [12, 13]. Also, we aim to establish the relation of structural relaxation behavior with macroscopic properties, i.e., the relationship between the change of elastic modulus and glass-forming ability (GFA), and plasticity of BMGs.

Various BMGs were prepared by arc-melting mixtures of the constituent elements under Ti-gettered argon atmosphere. Alloy ingots were then sucked into a water-cooled copper mold to prepare 1.5 × 4.0 × 45 mm glassy plates which were cut using a high-speed diamond/copper saw to obtain 40 mm long specimens. All specimens were ground and polished with abrasive papers to reduce the surface roughness. Glassy structures of the as-cast samples were verified by X-ray diffraction (XRD) with Cu K α radiation (λ = 0.15406 nm) and differential scanning calorimetry (DSC) with protection of argon at a flow rate of 60 mL/min and at a heating rate of 5 K/min.

Variation of Young's modulus with temperature was measured using impulse excitation technique (IET) (HT1600, IMCE, Belgium) [12]. A rectangle sample with a known dimension and mass is suspended at two nodes (namely, the zero-displacement points) of the first bending vibration mode in a dedicated IET furnace [14]. The vibration of the specimen can be excited by tapping its midpoint using a pneumatic tapper. Mechanical vibration generates sound wave which transmits along a ceramic bar inside the furnace and is detected by a high-precision microphone outside of the furnace. After the Fourier analysis of the sound wave, the frequency, as well as the

dimensions and mass of the specimen, is used to calculate the Young's modulus according to the American Society for Testing and Materials (ASTM) standard 1876 [15].

In general, Young's modulus of a crystalline material decreases (if phase transition does not occur) almost linearly with temperature [16]. In contrast, there are four stages of change with temperature in the typical *E*-*T* curve of BMGs, as shown in Fig. 1a. At Stage I, the Young's modulus decreases linearly with temperature, resembling those observed in crystalline solids. For crystalline solids, such a change is dominated by the anharmonic atomic vibration and can be well described by the Debye-Grüneisen (DG) model. The potential energy landscape (PEL) can be invoked to understand the temperature-dependence of the modulus as schematically indicated in Fig. 1b, and each basin in this landscape represents an inherent atomic structure. At Stage I, the basin occupancy is fixed and the temperature-dependence of the modulus at this stage is dominated by the anharmonic atomic vibration [17].

From 450 to 600 K (just below $T_g$), the change of Young's modulus with temperature becomes inappreciable, which features Stage II. Since BMGs are rapidly quenched from their melts, the relaxation during vitrification is insufficient, and the atomic system is frozen in a configuration that corresponds to a local minimum with relatively higher energy in the PEL. Therefore, when it is reheated, short-range atomic rearrangement can operate at the temperature below $T_g$. Such a relaxation can be comprehended using the notion of meta-basin reorganization, namely hopping among a number of local energy minima in the PEL [18, 19]. It is conceivable that the

quenched local atomic system has the tendency to hop into more stable configuration with the lower minimum energy, leading to the contribution of the local atomic rearrangement to the elastic modulus (i.e., the Born term [20]) and thus compensating the decreasing DG effect.

Stage III is featured by a sharp decrease of Young's modulus; and the glass transition point is determined by the intersection between the tendency lines near the end of Stage II and the start of Stage III, as indicated in Fig. 1a. In this stage, the BMG specimen begins to soften rapidly due to the production of large numbers of free volume [21] as well as the significant structural relaxation. In the following Stage IV, crystallization is detected based on the quick surge of Young's modulus.

To further understand the sub-$T_g$ relaxation of BMGs at Stage II, Fig. 1c depicts the variation of isothermal Young's modulus of Vitreloy 1 with time at 0.7, 0.74 and 0.78 $T_g$, respectively. The data were fitted with a stretched exponential function:

$$\frac{E_e - E}{E_e - E_{DG}} = e^{-((t+t_0)/\tau)^n} \quad (1)$$

where $\tau$ is the temperature-dependent characteristic relaxation time and follows the Arrhenius equation: $\tau = \tau_0 e^{Q/RT}$, $E$ is the Young's modulus at time $t$, $t_0$ is owing to the initial (partially relaxed) value of $E$, $E_e$ and $E_{DG}$ are the moduli at fully equilibrium state and non-relaxed state (given by the extrapolation of the DG model), respectively, and $n$ is the stretching exponent. The lower annealing temperature leads to the higher $E_e$ and the longer relaxation time to reach it. And the relation between $E_e$ and $T$ is still linear as shown in the inset of Fig. 1c once the basin occupancy no longer changes after a long-time aging. Fig. 1d shows the change of Young's modulus with

temperature for the as-cast and relaxed states of $Cu_{36}Zr_{48}Al_8Ag_8$ BMG, where the latter is obtained after annealing at $T_g$ for 20 min. The as-cast sample shows a platform in stage II, whereas the platform disappears after annealing. The modulus of the annealed sample varies linearly with temperature, indicating the applicability of the DG model if the atomic system, even though disordered, does not rearrange. This result could be associated with annealing-induced embrittlement in metallic glasses [22, 23], which indicates the relation between plasticity and sub-$T_g$ relaxation.

Heating the BMGs to the temperature around $T_g$ brings about α-relaxation, namely the atomic system tends to be ergodic. At this temperature the stress relaxation or viscous flow becomes also detectable, which however is not the cause of the sharp decrease of Young's modulus since the vibration period of the BMG specimen is still in the order of $10^{-3}$ s, which is a few orders smaller than the relaxation time at $T_g$ (typical value is 10-100 s) [24]. The fast reduction of Young's modulus should merely be attributed to the α-relaxation. Therefore, the rate of decrease of Young modulus at the temperature right above $T_g$, hereafter named the softening rate, indicates how quickly (in terms of temperature change) the atoms become alienated [25]. This notion inspires us to correlate the softening rate of modulus $(dE/dT)_{Tg}$ with the GFA since the latter is affected by the tendency of crystallization and the rate of atomic alienation.

Fig. 2a shows the sharp contrast of softening rates of Zr-based and La-based BMGs. The well-known Vitreloy 1 BMG has a very small softening rate of 115 MPa/K and an excellent GFA, indicated by the maximum casting diameter $d_c$ of about

50 mm [26], whilst the poor glass former LaNiAl with $d_c$ of 2 mm [27] has the larger softening rate of 210 MPa/K. Fig. 2b shows the relationship between softening rate $(dE/dT)_{Tg}$ and GFA for a variety of BMGs. It is apparent that the larger softening rate, indicating the higher rate of atomic alienation, should make crystallization easier and corresponds to a smaller GFA.

The relation between the softening rate of modulus and the alienation of atoms has been formulated by Knuyt based on the assumption of Gaussian radial distribution of atoms, which can be expressed as [28]: $d\ln G/dT \propto d\ln V_{\mathrm{at}}/dT$, where $V_{\mathrm{at}}$ is the average atomic volume, and $G$ is the shear modulus. With a small variation of Poisson's ratio, $\ln G$ is proportional to $\ln E$. The Knuyt's relation indicates that the larger softening rate is associated with the faster increase of average atomic volume. The temperature dependence of modulus above $T_{\mathrm{g}}$ can also be described by the rate of barrier crossing when the atomic system is sampling the PEL [29]. The larger barrier crossing rate implies that the atomic system tends to stay more often in shallower PEL basins, which corresponds to the larger softening rate and the higher tendency of crystallization. These understandings make us believe that the change of elastic modulus can serve as another efficient indicator, in addition to enthalpy (using DSC) or volume (using dilatometer), to explore the underlying relaxation dynamics of BMGs and further to understand the nature of glass formation.

When heating BMGs to the temperature about $0.7T_{\mathrm{g}}$, the DG effect becomes inappreciable, which is attributed to the change of atomic configurations as mentioned above. Since the temperature is well below $T_{\mathrm{g}}$, such a configuration change could only

be induced by local rearrangements of a small number of atoms, resembling the Johari-Goldstein $\beta$-relaxation [30], which is generally accompanied by significant changes of the physical properties of MGs [31-33]. Unlike mobile dislocations and other crystallographic defects in crystalline materials, the carriers of plastic deformation in MGs is associated with local atomic rearrangements [34]. Based on the elastic model [29, 35-37], the relaxation, glass transition and plastic deformation in MGs can all be considered as the phenomenon of flow and are activated by different processes, for instance, thermal or mechanical process to cross the energy barrier [29, 36]. Therefore, the activation energy barrier is a key factor for controlling the flow in MGs. The gentle slope in stage II as shown in Fig. 3a indicates that the significant local atomic rearrangements, which are the only possible relaxation mechanism at low temperature (below $T_g$), compensates the reduction of modulus induced by the DG effect. The slope change from stage I to stage II thus indicates the degree of the sub-$T_g$ relaxation. It is noted that local atomic rearrangements are also the plastic deformation mechanism at low temperature because there is no crystallographic defect in MGs. Therefore, the degree of sub-$T_g$ relaxation, as exhibited by the slope change form stage I to stage II, should have a close relation with the plasticity of a MG. The more severe is the sub-$T_g$ relaxation, the easier of their plastic flow and therefore the better plasticity it would exhibit.

The temperature and time dependence of modulus variation can be expressed as $E(T,t) = E_{DG}(T) + \Delta E_{sub}(T,t)$, where $\Delta E_{sub}(T,t)$ approaches the maximum value following the stretched exponential function. Therefore, the slope change from stage I

to stage II, as shown in Fig. 3a, can be given as $\left(dE/dT\right)_{II}-\left(dE/dT\right)_{I}=d\left\{\Delta E_{\mathrm{sub}}\left(T,\left(T-T_0\right)/\dot{T}\right)\right\}/dT$ with $T_0$ being the starting temperature of stage II. To have a fair comparison between different BMGs, we determine the slope change using the normalized modulus $\varepsilon=E/E_{T_g}$ and temperature $\theta=T/T_{\mathrm{g}}$. The non-dimensional slope change $\psi=\left(d\varepsilon/d\theta\right)_{II}-\left(d\varepsilon/d\theta\right)_{I}$, named the degree of sub-$T_{\mathrm{g}}$ relaxation, is plotted against the Poisson's ratio $\nu$ of the examined BMGs, since the Poisson's ratio is regarded as an effective indicator of plasticity [37], as shown in Fig. 3(b) .The least square linear fitting line (with a correlation coefficient about 0.88) roughly passes through the data with a slope of 0.29 ± 0.03. The data are clearly separated into two groups. Those BMGs with prominent sub-$T_{\mathrm{g}}$ relaxation are associated with larger $\nu$ (> 0.33) and generally possess good plasticity. On the other hand, those BMGs with unapparent sub-$T_{\mathrm{g}}$ relaxation possess smaller $\nu$ (< 0.33) and worse plasticity. The atomic system of BMG is vitrified during rapid cooling. When it is reheated, the quenched atomic system has the tendency to hop into a more stable configuration with lower energy after overcoming the energy barrier $\Delta Q$ [35], which can be related to $\psi$ as schematically shown in the insets of Fig. 3b. The BMG with the larger $\psi$ (> 0.1) should have the smaller $\Delta Q$, which can be easily surmounted via the addition of strain energy during deformation, leading to good plasticity. Conversely, the BMGs with a small $\psi$ (< 0.1) is difficult to rearrange during low-temperature deformation, resulting in brittleness.

In summary, an in-situ impulse excitation technique was used to carefully monitor the changes in the Young's modulus from room temperature to the

temperatures slightly above their $T_g$ for a variety of BMGs with different chemical systems. The variation of Young's modulus with temperature can be separated into four stages and a strong correlation between the softening rate of Young's modulus and GFA has been found. The smaller softening rate corresponds to better GFA. This correlation can be explained by the notion of atomic alienation. The higher softening rate indicates the higher tendency of alienation, which corresponds to easier crystallization and a smaller GFA. In addition, it is found that the slope change from stage I to stage II, namely the prominence of sub-$T_g$ relaxation, $\psi$, can well be correlated with the Poisson's ratio. This correlation suggests that the local atomic rearrangement is the main reason of good plasticity achieved in some BMG compositions and it also can explain the annealing-induced embrittlement, which annihilates the tendency of low-temperature rearrangement. Our current findings suggest that the in-situ measurement of high-temperature Young's modulus leads to a new predictive method for glass formation and deeper understanding of the relationship between macroscopic performance and atomic structure.

## Acknowledgements

This research was supported by the National Natural Science Foundation of China (Nos. 51371003, 51271212, 51531001, 51671018, 51422101 and U1530402), 111 Project (B07003), International S&T Cooperation Program of China (2015DFG52600) and the Program for Changjiang Scholars and Innovative Research Team in University (IRT_14R05). H. H. Ruan acknowledges the support from the

Early Career Scheme (ECS) of the Hong Kong Research Grants Council (No. 25200515, HK PolyU account F-PP27) and the General Research Funds (G-YBDH) of Hong Kong Polytechnic University.

## References


[1] A.L. Greer, Science 267 (1995) 1947.

[2] W.L. Johnson, Prog. Mater. Sci. 30 (1986) 81-134.

[3] A. Greer, M. Gibbs, J. Leake, J. Evetts, J. Non-Cryst. Solids 38 (1980) 379-384.

[4] T. Egami, Ann. N. Y. Acad. Sci. 371 (1981) 238-251.

[5] J. Bendert, A. Gangopadhyay, N. Mauro, K. Kelton, Phys. Rev. Lett. 109 (2012) 185901.

[6] H. Chen, E. Coleman, App. Phys. Lett. 28 (1976) 245-247.

[7] S. Bossuyt, S. Giménez, J. Schroers, J. Mater. Res. 22 (2007) 533-537.

[8] H. Chen, J. App. Phys. 49 (1978) 3289-3291.

[9] L. Huo, J. Zeng, W. Wang, C.T. Liu, Y. Yang, Acta Mater. 61 (2013) 4329-4338.

[10] J. Qiao, J. Pelletier, Intermetallics 19 (2011) 9-18.

[11] A. Slipenyuk, J. Eckert, Scr. Mater. 50 (2004) 39-44.

[12] G. Roebben, B. Bollen, A. Brebels, J. Van Humbeeck, O. Van der Biest, Rev. Sci. Instrum. 68 (1997) 4511-4515.

[13] E. Le Bourhis, P. Gadaud, J.-P. Guin, N. Tournerie, X. Zhang, J. Lucas, T. Rouxel, Scri. Mater. 45 (2001) 317-323.

[14] J. Wang, H. Ruan, X. Wang, J. Wan, J. Non-Cryst. Solids (2018).

[15] S. Astm, West Conshohocken: ASTM International (2003) 1876-1878.

[16] J.L. Murray, ASM international (1987) 340-345.

[17] F.H. Stillinger, P.G. Debenedetti, J. Phys. Chem. B 103 (1999) 4052-4059.

[18] M. Goldstein, J. Chem. Phys. 51 (1969) 3728-3739.

[19] P.G. Debenedetti, F.H. Stillinger, Nature 410 (2001) 259-267.

[20] J. Ashwin, E. Bouchbinder, I. Procaccia, Phys. Rev. E 87 (2013) 042310.

[21] F. Spaepen, Scr. Mater. 54 (2006) 363-367.

[22] Y. Yokoyama, T. Yamasaki, P.K. Liaw, A. Inoue, Acta Mater. 56 (2008) 6097-6108.

[23] P. Murali, U. Ramamurty, Acta Mater. 53 (2005) 1467-1478.

[24] J. Ketkaew, M. Fan, M.D. Shattuck, C.S. O'Hern, J. Schroers, Scr. Mater. 149 (2018) 21-25.

[25] R. Busch, E. Bakke, W.L. Johnson, Acta Mater. 46 (1998) 4725-4732.

[26] P. Gadaud, S. Pautrot, J. Non-Cryst. Solids 316 (2003) 146-152.

[27] A. Peker, W.L. Johnson, App. Phys. Lett. 63 (1993) 2342-2344.

[28] Z. Zhu, Y. Li, Z. Wang, X. Gao, P. Wen, H. Bai, K. Ngai, W.H. Wang, J. Chem. Phys. 141 (2014) 084506.

[29] G. Knuyt, L. Stals, L. De Schepper, W. De Ceuninck, Mater. Sci. Eng. A 133 (1991) 261-264.

[30] W.L. Johnson, K. Samwer, Phys. Rev. Lett. 95 (2005) 195501.

[31] Y. Liu, T. Fujita, D. Aji, M. Matsuura, M. Chen, Nat. Commun. 5 (2014) 3238.

[32] Q. Wang, J. Liu, Y. Ye, T. Liu, S. Wang, C. Liu, J. Lu, Y. Yang, Mater. Today 20 (2017) 293-300.

[33] L. Hu, Y. Yue, J. Phys. Chem. C 113 (2009) 15001-15006.

[34] H. Yu, X. Shen, Z. Wang, L. Gu, W.H. Wang, H. Bai, Phys. Rev. Lett. 108 (2012) 015504.

[35] W.H. Wang, Y. Yang, T. Nieh, C. Liu, Intermetallics 67 (2015) 81-86.

[36] J. Wang, W.H. Wang, Y. Liu, H. Bai, Phys. Rev. B 83 (2011) 012201.

[37] W.H. Wang, Prog. Mater. Sci. 57 (2012) 487-656.

## Captions

**Figure 1.** (a) Diagram of temperature dependence of Young's modulus for Vitreloy 1. Four stages, (I) Debye-Grüneisen thermal expansion effect of atomic vibrations, (II) Structure relaxation, (III) Glass transition regime and (IV) Crystallization, can be observed. (b) Schematic depictions of free energy basins for different landscape scenarios corresponding to Fig. 1(a). (c) Relaxation of Vitreloy 1 at 0.7, 0.74 and 0.78 $T_g$, respectively. The data are fitted according to Eq. (1) (solid red lines). (d) Diagram of modulus relaxation for stage II with respect to the annealing ones (green circles, annealing at $T_g$ for 20 min).

**Figure 2.** (a) Comparison Diagram of the softening rates for Vitreloy 1 and $La_{60}Al_{15}Ni_{25}$. (b) Relation between the maximum diameter $d_c$ and softening rate of modulus for a variety of BMGs. The solid red line is a fit following a power law equation: $(dE/dT)_{T_g} = k(d_c)^a$, where $a$ is the scaling exponent and $k$ is the allometric coefficient. (■ Zr-based, ▲ CuZr-based, ● Cu-based, ◆ Fe-based, ▶ RE-based, ⬟ Ni-based, see the Supporting Information for more details).

**Figure 3.** (a) Diagram of the degree of sub-$T_g$ relaxation from stage I to stage II. (b) Correlation between the Poisson's ratio $v$ and the degree of sub-$T_g$ relaxation, $\psi$, for different BMGs, The inserted diagram depicts the correlation between the degree of sub-$T_g$ relaxation and the energy barrier $\Delta Q$ in PEL. (■ Zr-based, ▲ CuZr-based, ● Cu-based, ◆ Fe-based, ▶ RE-based, see detail in Table S1 of Supporting Information).

Figure(1)
Click here to download high resolution image

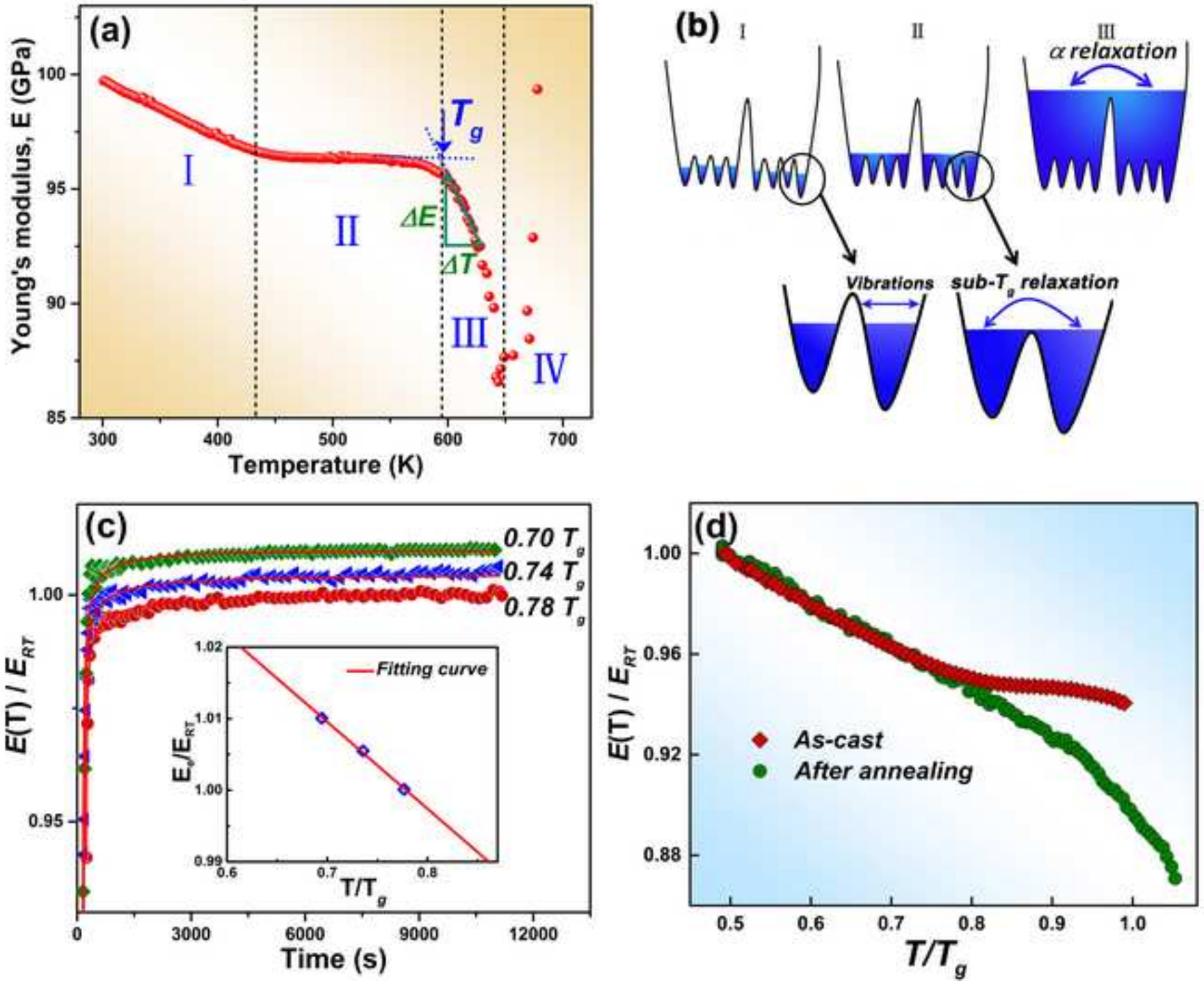

Figure(2)
Click here to download high resolution image

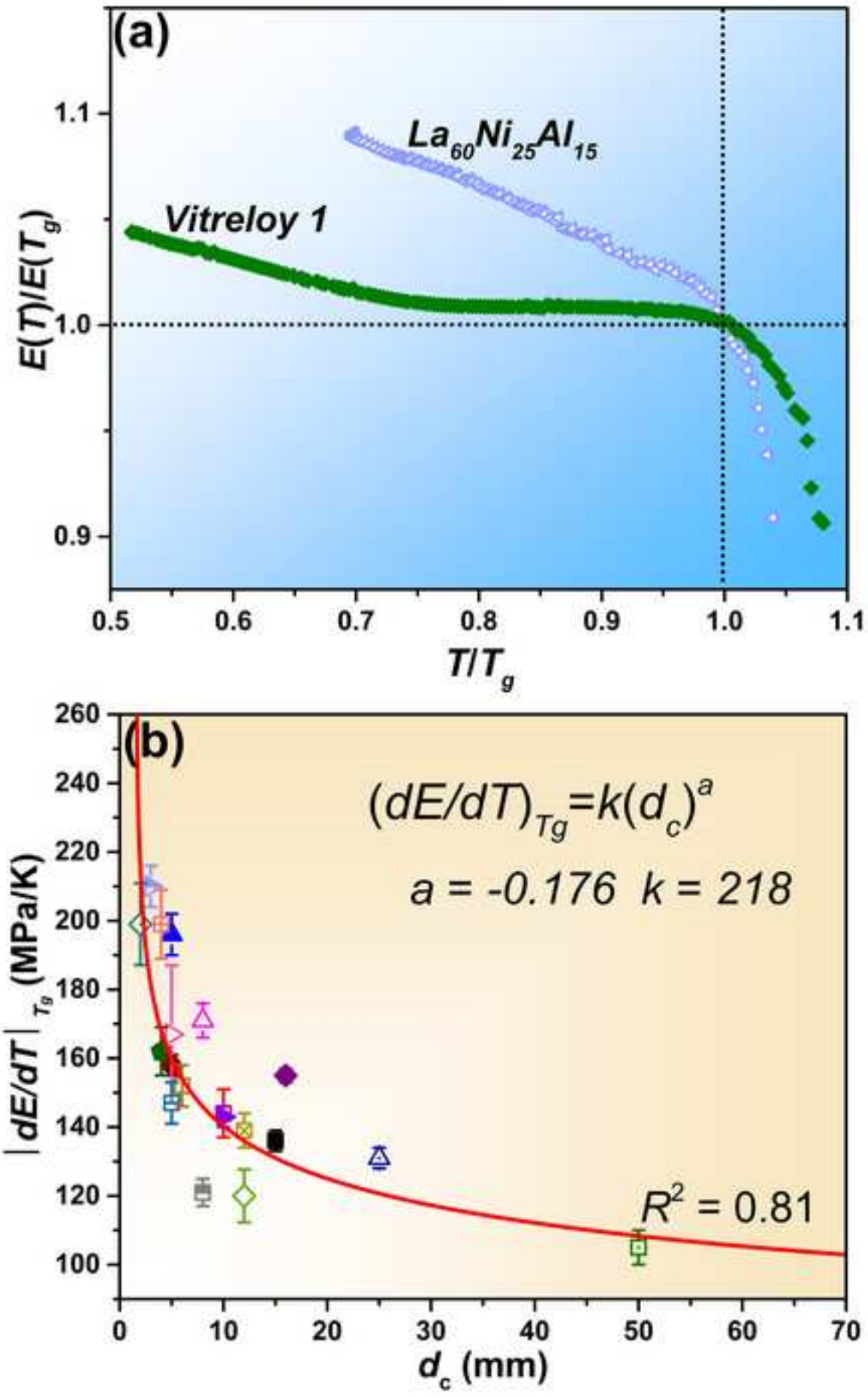

Figure(3)
Click here to download high resolution image